A preconditioner for linearized Navier-Stokes problem in exterior domains

Delphine Jennequin

INRIA

INSTITUT NATIONAL DE RECHERCHE EN INFORMATIQUE ET EN AUTOMATIQUE

A preconditioner for linearized Navier-Stokes problem in exterior domains

Delphine Jennequin

N° 5861

Mars 2006

Thème NUM

ISSN 0249-6399 ISRN INRIA/RR--5861--FR+ENG

A preconditioner for linearized Navier-Stokes problem in exterior domains

Delphine Jennequin

Thème NUM — Systèmes numériques
Projets SIMPAF

Rapport de recherche n 5861 — Mars 2006 — 22 pages

Abstract: We aim to approach the solution of the stationary incompressible Navier-Stokes equations in a three-dimensional exterior domain. Therefore, we cut the exterior domain by a sphere of radius R and we impose some suitable approximate boundary conditions (ABC) to the truncation boundary of the computational domain: the minimal requirement of these conditions is to ensure the solvability of the truncated system and the decay of the truncation error if R grows. We associate to the truncated problem a mesh made of homothetic layers, called exponential mesh, such that the number of degrees of freedom only grows logarithmically with R and such that the optimal error estimate holds. In order to reduce the storage, we are interested in discretizations by equal–order velocity–pressure finite elements with additional stabilization terms. Therefore, the linearisation inside a quasi–Newton or fixed–point method leads to a generalized saddle–point problem, that may be solved by a Krylov method applied on the preconditioned complete system matrix. We introduce a bloc–triangular preconditioner such that the decay rate of the Krylov method is independent of the mesh size h and we give an estimate for this rate in function of the truncation radius and of the Reynolds number. Some three-dimensional numerical results well confirm the theory and show the robustness of our method.

Key-words: Exterior domains, exponential mesh, saddle-point problems, preconditioning, Navier-Stokes equations

Unité de recherche INRIA Futurs
Parc Club Orsay Université, ZAC des Vignes,
4, rue Jacques Monod, 91893 ORSAY Cedex (France)
Téléphone : +33 1 72 92 59 00 — Télécopie : +33 1 72 92 59 ??

Un preconditionneur pour le problème de Navier–Stokes linéarisé dans un domaine extérieur

Résumé : Nous voulons approcher numériquement la solution des équations de Navier-Stokes stationnaires incompressibles dans un domaine extérieur tridimensionnel. Pour cela, nous tronquons notre domaine extérieur par une sphère de rayon R et imposons des conditions aux limites artificielles bien choisies sur le bord libre du domaine: elle doivent assurer au minimum que le problème soit bien posé et que l'erreur de troncature décroisse quand R devient grand. Nous associons à ce problème tronqué un maillage composé de couches homothétiques, appelé maillage exponentiel, de manière à ce que le nombre de degrés de liberté ne croisse que logarithmiquement avec R et que l'estimée d'erreur soit optimale. Pour des raisons évidentes de stockage, nous nous intéressons à une discrétisation par des éléments finis de même ordre pour la vitesse et la pression avec un terme supplémentaire de type stabilisation. Ceci implique que la linéarisation à l'intérieur d'itérations de quasi–Newton ou de point–fixe conduit à un problème de point selle généralisé, qui peut être résolu par une méthode de Krylov appliquée sur le système complet précondionné. Nous introduisons une préconditionneur triangulaire par bloc tel que le taux de convergence de la méthode de Krylov ne dépende pas de h, et nous donnons une estimation de ce taux en fonction du nombre de Reynolds et du rayon de troncature. Des resultats numériques tridimensionnels nous permettent de confimer la théorie et montrent la robustesse de la méthode.

Mots-clés : Domaines extérieurs, maillage exponentiel, problèmes de point-selle, preconditionnenement, équations de Navier-Stokes

1 Introduction

We are interested in the approximation of 3D stationary Navier–Stokes flows in an exterior domain with non–zero velocity at infinity. More precisely, the physical model writes:

$$\left\{\begin{array}{ll} -\frac{1}{\mathcal{R}e}\Delta\tilde{u} + (\tilde{u}\cdot\nabla)\tilde{u} + \nabla\pi = \Phi & \text{in } \Omega^c, \\ \operatorname{div}\tilde{u} = 0 & \text{in } \Omega^c, \\ \tilde{u}\,|\,\partial\Omega = 0, \quad \tilde{u}(x)\to e_1 \ (|x|\to\infty), & \end{array}\right.$$

where Ω is a bounded open set with compact Lipschitz boundary $\partial\Omega$ and with a connected complement Ω^c, $\mathcal{R}e$ is the Reynolds number, $\tilde{u}$ is the velocity, π is the pressure, and $e_1 = (1,0,0)$. We suppose that, if $\mathcal{R}e$ is small enough, $\tilde{u} - e_1$ decays as $O(|x|^{-1})$ as $|x|$ goes to infinity. After a change of variables, the system may be transformed into this problem:

$$\left\{\begin{array}{lll} -\Delta u + \mathcal{R}e\cdot D_1 u + \mathcal{R}e\cdot(u\cdot\nabla)u + \nabla p = F & \text{dans} & \overline{\Omega}^c, \\ \operatorname{div} u = 0 & \text{dans} & \overline{\Omega}^c, \\ u\,|\,\partial\Omega = -e_1, \quad u(x)\to 0 \ (|x|\to\infty), & & \end{array}\right. \tag{1}$$

where D_1 represents the first spatial derivative, and $u(x) = \kappa\tilde{u}(x/L) - e_1$, $p(x) = \frac{L}{\kappa^2}\mathcal{R}e\pi$. The resolution of this problem may be decomposed into several steps. At first, we approximate the original problem by a truncated problem on a domain of radius R with a suitable local approximate boundary condition (ABC) on the outer boundary. Approximate Boundary Conditions have interested many authors (see the review of Tsynkov [19]). The minimal requirement of an ABC is to ensure the solvability of the truncated problem and the decay of the truncation error as R goes to infinity. Moreover, for the discrete problem, R has to be large enough to reduce the truncation error to the level of the discretization error. Because of the important size of the computational domain, we have to define an appropriate graded mesh such that the number of degrees of freedom moderately grows with R. We denote h the size of the mesh near the obstacle. After that, we must find some finite elements adapted to the Navier–Stokes equations and adapted to exterior problems in the sense that the discretization must be uniformly LBB–stable in h and R. At last, we must find a solver for the nonlinear saddle–point problem resulting from the discretrization of the Navier–Stokes system. Such a solver consists of a nonlinear method and of a linear iterative method for linearized Oseen–type systems. The first steps have already been studied in [10, 6, 7] and we will focus on the last step.

Historically, this approach to solve exterior problems was introduced by Goldstein [14] to solve Poisson equation in Ω^c where Ω is a bounded set of $\mathbb{R}^3$. The system considered in [14] reads:

$$-\triangle u = f \text{ in } \Omega^c, \quad u = g \text{ on } \partial\Omega, \quad \frac{\partial u}{\partial r} + \frac{1}{r}u = o(\frac{1}{r}) \text{ as } r\to\infty,$$

where f and g are smooth functions and f has a bounded support in Ω^c. This system is written in polar coordinates and $r = |x|$ represents the distance to the original point. This problem is replaced by the approximate truncated problem on $\Omega_R = \Omega^c \cap B(O,R)$ with Robin-type boundary conditions on the free boundary:

$$-\triangle u = f \text{ in } \Omega_R, \quad u = g \text{ on } \partial\Omega, \quad \frac{\partial u}{\partial r} + \frac{1}{r}u = 0 \text{ on } \partial\Omega_R \setminus \partial\Omega.$$

The truncated problem is solved by a finite element method and we obtain an approximate discrete solution u_h^R for each $h > 0$. When the mesh size h is quasi-uniform, the number of unknowns increases like $O(R^3)$. A quasi-uniform mesh is introduced such that the optimal error estimate holds and the number of equations is bounded by Ch^{-3} with C independent of h and R. Moreover, for Pk finite elements, it is proved that the optimal error estimate holds for $h^k \approx R^{-3/2}$. Alouges [2] introduces an approach, mixing infinite elements of Ying [22] and the method of Goldstein to solve the following problem of micromagnetics

$$\triangle u = 0 \in \Omega^c, \quad \triangle u = \nabla\cdot v \text{ in } \Omega, \quad [\frac{\partial u}{\partial n}] = v\cdot n \text{ across } \partial\Omega,$$

where Ω is convex, v is a given function, n is the outward unit normal of $\partial\Omega$ and $[\,]$ denotes the jump across $\partial\Omega$. He uses a finite element method coupling a finite mesh in Ω and a graded mesh for Ω^c composed of homothetic layers: the construction of this kind of mesh leads to low cost of storage, since matrices needs only to be build on the first layer. Moreover, a change of variables makes the rigidity matrix a almost bloc-Toeplitz matrix which

is well balanced and acts as a preconditioner. At last, the Robin-type boundary conditions on the outer free boundary are proved to be more efficient than Dirichlet or Neumann ones. In [1], Alouges, Mefire and Laminie used the same homothetic layers and their storage property to solve the problem

$$\nabla \wedge H = 0 \text{ in } \mathbb{R}^3, \quad \nabla \cdot (\mu(H + H^s)) = 0 \text{ in } \mathbb{R}^3, \quad |H(x)| \to 0 \text{ as } |x| \to \infty,$$

where H^s is the magnetic source field, H is the magnetic reaction field and μ is the permeability of the material. The truncated problem is solved by edge elements and they use Dirichlet and Neumann boundary conditions on the outer truncation boundary. The error estimate depends on the interior mesh size, on the number of homothetic layers and on the homothetic coefficient of the exponential mesh. Some preconditioning techniques for exterior problems are also presented. In [8] and [9], Deuring considers the Stokes system

$$-\triangle u + \nabla p = f \text{ in } \Omega^c, \quad \nabla \cdot u = 0 \text{ in } \Omega^c, \quad u = 0 \text{ on } \partial\Omega, \quad u(x) \to 0 \text{ as } |x| \to \infty,$$

where Ω is a bounded domain with connected Lipschitz boundary, u is the velocity and p is the pressure. The author considers the truncated exterior domain $\Omega^c \cap B(O, R)$ and introduces an artificial boundary condition on the outer boundary. The truncation error decays as $R^{-3/2}$ and some discretization error estimates are given. Moreover, the author proves that the Mini element (P1+bubble-P1) satisfies the Babuska-Brezzi condition with a constant independent of R.

Concerning our problem (9), Deuring et al introduce in [10] a suitable approximate boundary condition under a smallness assumption on $\mathcal{R}e$: indeed, they prove that the truncation error for the continuous problem decays as $O(R^{-1})$ as R goes to infinity under some suitable assumption on f and $\mathcal{R}e$. Then, in [6] and [7], Deuring gives an estimate of the discretization error for the truncated problem of (9) associated with the ABC given in [10]. This estimate may be written as follows: if we denote $(u_{h,R}, p_{h,R})$ the solution of the truncated problem discretized by P1-P1 finite elements with the stabilization term introduced by Rebollo in [17], the total error is given by

$$\|\nabla(u - u_{h,R})\|_2 + \|(p - p_{h,R})_{|B(O,s)\cap\Omega^c}\|_2 \leq C(h \ln(R/s) + h^t + R^{-1}), \tag{2}$$

where (u, p) is the solution of the original problem, s is the radius of a vicinity of Ω in where we want to approximate precisely the solution, $t \in]0, 1]$ depends on the regularity of the solution near Ω. This relation is valid if $\mathcal{R}e$ is small enough and if there is a constant μ such that $hR \leq \mu$. We use the same ABC and the same dicretization as Deuring in [10, 3, 6, 7] and we decompose the computational domain into homothetic layers, so that our framework is similar to the one of Goldstein [14] and Alouges [2] that we will describe above.

This discretization leads to a nonlinear discrete variational problem of the form

$$\begin{cases} \text{Find } (u_{h,R}, p_{h,R}) \in V_{h,R} \times Q_{h,R} \text{ such that} \\ d(u_{h,R}, u_{h,R}, v_{h,R}) + b(v_{h,R}, p_{h,R}) = (f, v_{h,R}), & \forall v_{h,R} \in V_{h,R}, \\ b(u_{h,R}, q_{h,R}) - c(p_{h,R}, q_{h,R}) = (g, q_{h,R}), & \forall q_{h,R} \in Q_{h,R}, \end{cases} \tag{3}$$

where $V_{h,R}$ and $Q_{h,R}$ are the finite element spaces for the velocity and pressure, d, b, c are respectively some trilinear and bilinear h-uniformly continuous forms on $V_{h,R}^3$, $V_{h,R} \times Q_{h,R}$ and $Q_{h,R}^2$ defined in (24) (27) (18) and where c represents the pressure stabilization term. We choose to apply some quasi–Newton nonlinear iterations, so that, at each nonlinear step, we must solve the generalized saddle–point problem:

$$\begin{cases} \text{Find } (u_{h,R}, p_{h,R}) \in V_{h,R} \times Q_{h,R} \text{ such that} \\ a(u_{h,R}, v_{h,R}) + b(v_{h,R}, p_{h,R}) = (f, v_{h,R}), & \forall v_{h,R} \in V_{h,R}, \\ b(u_{h,R}, q_{h,R}) - c(p_{h,R}, q_{h,R}) = (g, q_{h,R}), & \forall q_{h,R} \in Q_{h,R}, \end{cases} \tag{4}$$

where $\forall u_{h,R}, v_{h,R} \in V_{h,R},\ a(u_{h,R}, v_{h,R}) = d(w_{h,R}, u_{h,R}, v_{h,R})$, $w_{h,R}$ resulting from the last nonlinear iteration. Then, a is a bilinear form, h-uniformly continuous and h-uniformly coervice in $V_{h,R}^2$. The matricial formulation of (4) writes

$$\begin{pmatrix} \boldsymbol{A} & \boldsymbol{B}^T \\ \boldsymbol{B} & -\boldsymbol{E} \end{pmatrix} \begin{pmatrix} U \\ P \end{pmatrix} = \begin{pmatrix} F \\ G \end{pmatrix}, \tag{5}$$

where $\boldsymbol{A}$ is a non–symmetric convection–diffusion matrix, $\boldsymbol{B}$ is the divergence matrix and $\boldsymbol{E}$ is a symmetric semi–definite positive stabilization matrix. There are two main classes of methods to solve saddle point problems: Uzawa methods and bloc–triangular or bloc–diagonal preconditioning of the complete problem inside a Krylov method. Both methods require a preconditioner for the convection–diffusion matrix and for the Schur complement matrix $\boldsymbol{S} = \boldsymbol{E} + \boldsymbol{B}\boldsymbol{A}^{-1}\boldsymbol{B}^T$. We will consider in this paper a bloc–triangular preconditioner inside

some FGMRES iterations. For problems issue from discretization of PDE, the cost of the method in function of the mesh size has to be studied. The point is that the number of iterations must be independent of the mesh size for bounded cases. For unbounded domains, we must take into account the influence of the truncation radius. The usual way to precondition the Schur complement $\boldsymbol{S}$ is to find a matrix easy to build and easy to inverse that is spectrally equivalent to $\boldsymbol{S}$ (i.e. a matrix $\tilde{\boldsymbol{S}}$ such that the spectral bounds of $\tilde{\boldsymbol{S}}^{-1}\boldsymbol{S}$ are independent of h). Many results are known for stable discretizations (with $\boldsymbol{E} = \boldsymbol{0}$) (for example, see [12, 18, 11]). For generalized saddle–point problems ($\boldsymbol{E} \neq \boldsymbol{0}$), the literature is less rich. However, Cao [5] prove that if

$$\begin{pmatrix} \boldsymbol{A} & \boldsymbol{0} \\ \boldsymbol{B} & \tilde{\boldsymbol{S}} \end{pmatrix}^{-1} \tag{6}$$

is a preconditioner for the complete system and if $\tilde{\boldsymbol{S}}$ is spectrally equivalent to $\boldsymbol{S}$, then the GMRES iteration count is independent of the mesh size. Moreover, in [4], the authors analyze the influence of the preconditioner inside FGMRES iterations when the Navier–Stokes equations are discretized with Rebollo stabilization. For the 3D-lid driven cavity benchmark, performances and eigenvalues analysis are similar to those of literature for 2D test–cases [12, 21, 18, 11, 16, 15]. In [4], all the constants are explicitly given, so that the framework may be used for exterior domains. In this work, we use the preconditioner introduced in [4] and we focus on the influence of the truncation radius.

This paper is divided in four parts. In Section 2, we present the physical model. The graded mesh based on homothetic layers is defined and we explicit the artificial Robin-type boundary condition. The stabilization technique is described and we introduce the discrete variational formulation of our exterior Navier–Stokes problem. In Section 3, we exhibit the continuity and coercivity bounds in function of $h, \mathcal{R}e$ and R. We prove that the discretization satisfies a generalized inf–sup condition with a stability constant independent of h and R. This condition is necessary to apply the results of [4]. Section 4 is devoted to preconditioning and we give spectral bounds of the preconditioned algebraic system. The results derive from [4] but we focus on the truncation radius R. We prove that the upper bound of the spectrum is bounded independently on $\mathcal{R}e, h$ and R. The lower bound is only independent on h. If R is supposed to be constant, the dependence in the Reynolds number is the same as in literature [15]: indeed, we show that the spectral lower bound decays as $O(\mathcal{R}e^{-4})$, and only as $O(\mathcal{R}e^{-2})$ if the SUPG-like velocity stabilization term is dropped. If $\mathcal{R}e$ is fixed, we obtain a decay as $O(R^{-2})$ for the lower bound. In Section 5, we show some numerical results in three-dimensional exterior domains. At first, we exhibit the eigenvalues of the preconditioned and non preconditioned problem. Without preconditioning, the spectral lower bound decays with h and the upper bound increase exponentially with R. When we use our preconditioner, we observe that the numerical results are better than predicted by theory: the FGMRES iteration count is almost independent of R and the dependence on the Reynolds number is similar to the bounded case [4]. After that, we study the performances of the solver. At last, we plot the solution for a physical test–case.

2 Model and discretization

We consider a sphere moving without rotation in an incompressible fluid. The body is represented by the polyhedral open domain $\hat{\Omega} \subset \mathbb{R}^3$. We choose as zero point the barycenter of the solid. Such a motion is modeled by the Navier-Stokes equations with homogeneous Dirichlet boundary conditions on the sphere boundary $\partial\hat{\Omega}$ and with a non-zero velocity at infinity. These equations write

$$\left\{ \begin{array}{l} -\nu\Delta v \ + \ (v\cdot\nabla)v \ + \ \nabla\pi \ = \ \Phi, \quad \mathrm{div}\, v \ = \ 0 \quad \text{in } \hat{\Omega}^c = \mathbb{R}^3\backslash\overline{\hat{\Omega}}, \\ \quad v \,|\, \partial\hat{\Omega} = 0, \quad v(x) \to \kappa\cdot e_1 \ \ (|x| \to \infty), \end{array} \right. \tag{7}$$

where $e_1 = (1,0,0)$, ν is the kinematic viscosity and $\kappa \in (0,\infty)$ is the velocity at infinity. The source term $\Phi : \mathbb{R}^3\backslash\overline{U} \mapsto \mathbb{R}^3$ is given. The unknowns v and π represent the velocity and the pressure. We put as characteristic length the radius L of the body and for the reference velocity, we choose the velocity at infinity κ. Put $v(x) := \kappa\tilde{u}(\tilde{x}) = \kappa\tilde{u}(x/L)$. The dimensionless formulation of (7) reads

$$\left\{ \begin{array}{ll} -\Delta\tilde{u} \ + \ \mathcal{R}e\,(\tilde{u}\cdot\nabla)\tilde{u} \ + \ \nabla\tilde{p} \ = \ \tilde{\Phi} & \text{in } \Omega^c \\ \mathrm{div}\,\tilde{u} \ = \ 0 & \text{in } \Omega^c, \\ \tilde{u} \,|\, \partial\Omega = 0, \quad \tilde{u}(\tilde{x}) \to e_1 \ \ (|\tilde{x}| \to \infty), & \end{array} \right. \tag{8}$$

where the domain Ω is the homothetic of radius 1 of $\hat{\Omega}$, $\mathcal{R}e = \frac{\kappa L}{\nu}$ is the Reynolds number and $\tilde{p} = \frac{L}{\kappa^2}\mathcal{R}e\,\pi$. Put $x := \tilde{x}$ for more simplicity. If $\tilde{u}$ is solution of (8), then $(u,p) := (\tilde{u} - e_1, \tilde{p})$ is solution of:

$$\left\{ \begin{array}{lll} -\Delta u \;+\; \mathcal{R}e\;\; D_1 u \;+\; \mathcal{R}e\,(u\cdot\nabla)u \;+\; \nabla p \;=\; F & \text{in} & \overline{\Omega}^c, \\ \operatorname{div} u \;=\; 0 & \text{in} & \overline{\Omega}^c, \\ u\,|\,\partial\Omega \;=\; -e_1, \quad u(x)\to 0 \;\; (|x|\to\infty), & & \end{array} \right. \tag{9}$$

where D_1 is the first spatial derivative.

We will now describe the exponential mesh introduced by Goldstein [14]. We choose $s \in]1,\infty[$ and we suppose that $\Omega_s := B(0,s)\setminus\overline{\Omega}$ is a vicinity of Ω in where we want a precise approximation of the exterior flow (u,p) solution of (9). We choose

$$h \in (0, s/2), R \in (4s, \infty). \tag{10}$$

We consider the truncated domain $\Omega_{h,R}$ whose boundary is the polyhedron $\Gamma_{h,R}$ and such that

$$B(0, R(1-h^2/s^2)^{1/2})\setminus\overline{\Omega} \subset \Gamma_{h,R} \subset B(0,R)\setminus\overline{\Omega}.$$

Moreover, we impose that the nodes of the truncation polyhedron belong to the sphere $B(0,R)$. We denote $\mathcal{T}_{h,R} = (K_l)_{1\le l\le k} = (K_l^{h,R})_{1\le l\le k_{h,R}}$ the partition of $\Omega_{h,R}$ where the elements K_l are some tetrahedrons. Moreover, we suppose that this partition can be decomposed into homothetic layers $(U_j)_{1\le j\le J}$ such that:

$$U_0 := \Omega_s, \quad U_j := B(0, 2^j\cdot s)\setminus B(0, 2^{j-1}\cdot s), \forall 1 \le j \le N, \tag{11}$$

and such that the diameter of each tetrahedron K_l with $K_l \cap U_j \neq \emptyset$ is of order $2^j h$ for all $j \in \{1,\cdots,J\}$. Then, the number of nodes of $\mathcal{T}_{h,R}$ grows only logarithmically with the truncation radius R (see [14]). Let h_K the diameter of K for all $K \in \mathcal{T}_{h,R}$. The regularity σ_K of K is defined by

$$\sigma_K^{-1} = \sup\{\text{ diam }(B);\ \text{B is a ball included in } K\}/h_K.$$

We suppose that this triangulation is regular (see [13, Appendix A.1]) in the sense that there is a constant σ such that

$$\forall K \in \mathcal{T}_{h,R}, \quad \sigma_K \le \sigma.$$

We choose as boundary condition on the truncation boundary $\Gamma_{h,R}$ the artificial boundary condition introduced

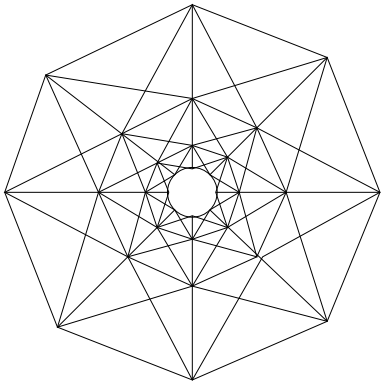

Figure 1: 2D projection of the exponential mesh.

in [10] and defined by

$$\sum_{j=1}^{3}(D_j v_k - \delta_{jk}\cdot p - \frac{\mathcal{R}e}{2}\cdot v_j\cdot v_k)(x)\cdot n_j^{h,R}(x) \;+\; \big(R^{-1} + \frac{\mathcal{R}e}{2}\cdot(1-n_1^{h,R}(x))\big)\cdot v_k(x) \;=\; 0, \tag{12}$$

for $1\le k\le 3,\ x\in\Gamma_{h,R}$, where $n^{h,R}$ is the unit outward normal on $\Omega_{h,R}$. We define now the classical Sobolev spaces. Let $\boldsymbol{H}_0^1(\Omega_{h,R}) = \big(H_0^1(\Omega_{h,R})\big)^3$, $\boldsymbol{H}^1(\Omega_{h,R}) = \big(H^1(\Omega_{h,R})\big)^3$ and $\boldsymbol{H}^{-1}(\Omega_{h,R})$ the dual of $\boldsymbol{H}_0^1(\Omega_{h,R})$. We denote $\|\quad\|_p$ the usual L^p-norm and $(\ ,\ )$ the L^2 scalar product. At last, we denote $|\quad|_1$ the usual semi–norm of $H^1(\Omega_{h,R})$, i.e. $\forall v\in\boldsymbol{H}^1(\Omega_{h,R}), |v|_1 = \|\nabla v\|_2$. We introduce the inner product defined on $\boldsymbol{H}^1(\Omega_{h,R})$ by

$$\forall u_{h,R}, v_{h,R}\in\boldsymbol{H}^1(\Omega_{h,R}), \quad (u_{h,R}, v_{h,R})_{h,R} := (\nabla u_{h,R}, \nabla v_{h,R}) + R^{-1}(u_{h,R|\Gamma_{h,R}}, v_{h,R|\Gamma_{h,R}}), \tag{13}$$

and the associated norm $\| \ \|^{(h,R)}$

$$\forall v_{h,R} \in \boldsymbol{H}^1(\Omega_{h,R}), \quad \| v_{h,R} \|^{(h,R)} := \Big(\| \nabla v_{h,R} \|_2^2 + R^{-1} \| v_{h,R_{|\Gamma_{h,R}}} \|_2^2 \Big)^{1/2}. \tag{14}$$

We discretize by equal–order finite elements with the stabilization introduced by Rebollo in [17]. We put

$$V_{h,R} = \{ v \in C^0(\overline{\Omega_{h,R}})^3 : v|K_l \in P_1(K_l)^3 \ \forall K_l \in \mathcal{T}_{h,R} \}, \tag{15}$$

$$Q_{h,R} = \{ p \in C^0(\overline{\Omega_{h,R}}) : p|K_l \in P_1(K_l) \ \forall K_l \in \mathcal{T}_{h,R} \}. \tag{16}$$

Writing $\lambda_{1,K}, \cdots, \lambda_{4,K}$ for the standard basis functions of the P1 finite element on $K \in \mathcal{T}_{h,R}$, the basis bubble function $\hat{b}_K$ on K is the polynomial of degree 4 defined by $\hat{b}_K = \lambda_{1,K} \cdots \lambda_{4,K}$. The bubble function space is defined by

$$B_{h,R} = \Big\{ v \in C^0(\overline{\Omega_{h,R}}), \text{ such that } \ v_{|K} \in \text{span}\,(\hat{b}_K), \forall K \in \mathcal{T}_{h,R} \Big\}.$$

Let $a_{1,h,R}, a_{2,h,R}$ two bilinear forms on $V_{h,R} \times V_{h,R}$, and assume that there are some constants α_1, α_2, $B_{1,h}, B_2 > 0$ such that for $v_{h,R}, w_{h,R} \in V_{h,R}$,

$$|a_{1,h,R}(v_{h,R}, w_{h,R})| \le B_{1,h,R} \, | v_{h,R} |_1 \, | w_{h,R} |_1 , \quad a_{1,h,R}(v_{h,R}, v_{h,R}) \ge \alpha_1 \, | v_{h,R} |_1^2 , \tag{17}$$

$$|a_{2,h,R}(v_{h,R}, w_{h,R})| \le B_2 \, | v_{h,R} |_1 \, | w_{h,R} |_1 , \quad a_{2,h,R}(v_{h,R}, v_{h,R}) \ge \alpha_2 \, | v_{h,R} |_1^2 . \tag{18}$$

Note that the constants α_1, α_2 and B_2 must be independent on h and R. We define Riesz operators $R_{1,h,R}, R_{2,h,R} : \boldsymbol{H}^{-1}(\Omega_{h,R}) \to \boldsymbol{H}_0^1(\Omega_{h,R})$ as follows: for $i \in \{1, 2\}, \varphi \in \boldsymbol{H}^{-1}(\Omega_{h,R})$, let $R_{i,h,R}\varphi$ be the unique element in $B_{h,R}^3$ that satisfies

$$a_{i,h,R}(R_{i,h,R}\varphi, v) = \varphi(v) \quad \forall v \in B_{h,R}^3;$$

see [17, p. 288]. Some explicit formulations are given in Appendix A.

Let $S : \boldsymbol{H}^1(\Omega_{h,R}) \times \boldsymbol{H}^1(\Omega_{h,R}) \to \boldsymbol{H}^{-1}(\Omega_{h,R})$ the continuous bilinear form defined by

$$\begin{aligned} &\forall u_{h,R}, w_{h,R}, v_{h,R} \in V_{h,R}, \quad \langle S(u_{h,R}, v_{h,R}), w_{h,R} \rangle := \mathcal{R}e \int_{\Omega_{h,R}} D_1 v_{h,R} \cdot w_{h,R} \, dx - \frac{\mathcal{R}e}{2} \int_{\Gamma_{h,R}} v_{h,R} \, w_{h,R} n_1^{h,R} \, dS \\ &+\mathcal{R}e \int_{\Omega_{h,R}} (\, (u_{h,R} \cdot \nabla) v_{h,R} \cdot w_{h,R} + \frac{1}{2} (\text{div}\, u_{h,R}) \, v_{h,R} \cdot w_{h,R} \,) \, dx \\ &-\frac{\mathcal{R}e}{2} \int_{\Gamma_{h,R}} (u_{h,R} \cdot n^{(h,R)}) v_{h,R} \cdot w_{h,R} \, dS. \end{aligned} \tag{19}$$

We introduce now the following discrete trilinear and bilinear forms

$$\begin{aligned} &\forall u_{h,R}, v_{h,R}, w_{h,R} \in V_{h,R}, \quad a_{h,R}^{(+)}(w_{h,R})(u_{h,R}, v_{h,R}) := \int_{\Omega_{h,R}} (\nabla u_{h,R} \cdot \nabla v_{h,R}) \, dx \\ &+ \int_{\Gamma_{h,R}} (\frac{1}{R} + \frac{\mathcal{R}e}{2}) u_{h,R} v_{h,R} \, dS + a_{1,h,R}\big(R_{1,h,R} S(w_{h,R}, u_{h,R}), R_{1,h,R} S(w_{h,R}, v_{h,R})\big), \end{aligned} \tag{20}$$

$$\forall u_{h,R}, v_{h,R}, w_{h,R} \in V_{h,R}, \quad a_{h,R}^{(-)}(u_{h,R})(v_{h,R}, w_{h,R}) := \langle S(u_{h,R}, v_{h,R}), w_{h,R} \rangle, \tag{21}$$

$$\forall u_{h,R} \in V_{h,R}, \quad \forall p_{h,R} \in Q_{h,R}, \quad b_{h,R}(u_{h,R}, p_{h,R}) = \int_{\Omega_{h,R}} p_{h,R} \nabla \cdot w_{h,R} \, dx, \tag{22}$$

and

$$\forall p_{h,R}, q_{h,R} \in Q_{h,R}, \quad c_{h,R}(p_{h,R}, q_{h,R}) = a_{2,h,R}(R_{2,h,R} \nabla p_{h,R}, R_{2,h,R} \nabla q_{h,R}). \tag{23}$$

The trilinear form d introduced in (3) is given by

$$\forall u_{h,R}, v_{h,R}, w_{h,R} \in V_{h,R}, \quad d(w_{h,R}, u_{h,R}, v_{h,R}) = a_{h,R}^{(+)}(w_{h,R})(u_{h,R}, v_{h,R}) + a_{h,R}^{(-)}(w_{h,R})(u_{h,R}, v_{h,R}). \tag{24}$$

We take, as discretization in $\Omega_{h,R}$ of the problem (9) with the boundary condition (12) on the truncation radius, the following nonlinear variational problem:

$$\left\{\begin{array}{l} \text{Find} \quad u_{h,R} \in V_{h,R}, \quad p_{h,R} \in Q_{h,R} \quad \text{with} \quad u_{h,R_{|\partial\Omega}} = -e_1 \text{ such that} \\ \forall\, v_{h,R} \in V_{h,R} \text{ with } v_{h,R_{|\partial\Omega}} = 0, \quad \forall\, q_{h,R} \in Q_{h,R}, \\ a^{(+)}_{h,R}(u_{h,R})(u_{h,R}, v_{h,R}) + a^{(-)}_{h,R}(u_{h,R})(u_{h,R}, v_{h,R}) - b_{h,R}(v_{h,R}, p_{h,R}) = l(v_{h,R}), \\ -b_{h,R}(u_{h,R}, q_{h,R}) - c_{h,R}(p_{h,R}, q_{h,R}) = 0. \end{array}\right. \tag{25}$$

The nonlinear problem is solved using the 'adaptive fixed–point defect correction method' [20], so that at each nonlinear iteration, we must solve the linear Oseen-type system with homogeneous Dirichlet boundary conditions:

$$\text{For } w_{h,R} \in V_{h,R} \text{ given such that } w_{h,R_{|\partial\Omega}} = -e_1, \tag{26}$$

$$\text{Find } (u_{h,R}, p_{h,R}) \in V_{h,R} \times Q_{h,R}, u_{h,R_{|\partial\Omega}} = 0 \text{ such that:}$$

$$\left\{\begin{array}{l} \forall (v_{h,R}, q_{h,R}) \in V_{h,R} \times Q_{h,R}, \quad v_{h,R_{|\partial\Omega}} = 0 \\ a^{(+)}_{h,R}(w_{h,R})(u_{h,R}, v_{h,R}) + a^{(-)}_{h,R}(w_{h,R})(u_{h,R}, v_{h,R}) - b_{h,R}(v_{h,R}, p_{h,R}) = \langle f, v_{h,R}\rangle \\ -b_{h,R}(u_{h,R}, q_{h,R}) - c_{h,R}(p_{h,R}, q_{h,R}) = \langle g, p_{h,R}\rangle, \end{array}\right. \tag{27}$$

where $w_{h,R} \in V_{h,R}, f \in V'_{h,R}, g \in Q'_{h,R}$ are defined in the previous iteration step of the nonlinear method.

3 Properties of the bilinear forms

In this section, the constants $C_1, C_2, ...$ are supposed independent of h, R and $\mathcal{R}e$. At first, we recall the Sobolev inequalities for unbounded domains. There exist two constants $C_1 > 0$ and $C_2 > 0$ such that $\forall h > 0, \forall R > 0$, we have

$$\forall w_{h,R} \in \boldsymbol{H}^1(\Omega_{h,R}), \quad \| w_{h,R} \|_6 \leq C_1 \| w_{h,R} \|^{(h,R)}, \tag{28}$$

and

$$\forall w_{h,R} \in \boldsymbol{H}^1(\Omega_{h,R}), \quad \| w_{h,R} \|_2 \leq C_2 R \| w_{h,R} \|^{(h,R)}. \tag{29}$$

We deduce that, using interpolation inequality,

$$\forall w_{h,R} \in \boldsymbol{H}^1(\Omega_{h,R}), \quad \| w_{h,R} \|_3 \leq C_3 R^{1/2} \| w_{h,R} \|^{(h,R)}. \tag{30}$$

Integrating by parts, we observe that

$$\begin{array}{l} \mathcal{R}e \displaystyle\int_{\Omega_{h,R}} ((u_{h,R} \cdot \nabla) v_{h,R} \cdot w_{h,R} + \frac{1}{2} (\operatorname{div} u_{h,R})\, v_{h,R} \cdot w_{h,R}\,)\, dx \\ -\dfrac{\mathcal{R}e}{2} \displaystyle\int_{\Gamma_{h,R}} (u_{h,R} \cdot n^{(h,R)}) v_{h,R} \cdot w_{h,R}\, dS = \\ \dfrac{\mathcal{R}e}{2} \displaystyle\int_{\Omega_{h,R}} (u_{h,R} \cdot \nabla v_{h,R}) w_{h,R} - (u_{h,R} \cdot \nabla w_{h,R}) v_{h,R}\, dx. \end{array} \tag{31}$$

Hence, we deduce that $\forall u_{h,R}, v_{h,R}, w_{h,R} \in V_{h,R}$,

$$\begin{aligned} |a^{(-)}_{h,R}(u_{h,R})(v_{h,R}, w_{h,R})| &\leq \mathcal{R}e \ \| D_1 v_{h,R} \|_2 \ \| w_{h,R} \|_2 + \frac{\mathcal{R}e}{2} \| v_{h,R_{|\Gamma_{h,R}}} \|_2 \ \| w_{h,R_{|\Gamma_{h,R}}} \|_2 \\ &\quad + \frac{\mathcal{R}e}{2} \| u_{h,R} \|_3 \ \| \nabla v_{h,R} \|_2 \ \| w_{h,R} \|_6 + \frac{\mathcal{R}e}{2} \| u_{h,R} \|_3 \ \| \nabla w_{h,R} \|_2 \ \| v_{h,R} \|_6 \\ &\leq C_2 R \| v_{h,R} \|^{(h,R)} \| w_{h,R} \|^{(h,R)} + C_1 C_3 \mathcal{R}e R^{1/2} \| u_{h,R} \|^{(h,R)} \| v_{h,R} \|^{(h,R)} \| w_{h,R} \|^{(h,R)} \\ &\leq C_4 \big(\mathcal{R}e\ R + \mathcal{R}e\ R^{1/2} \| u_{h,R} \|^{(h,R)}\big) \| v_{h,R} \|^{(h,R)} \| w_{h,R} \|^{(h,R)}. \end{aligned} \tag{32}$$

Lemma 1 *There exists a constant $C_5 > 0$ such that*

$$\forall \hat{w}_{h,R} \in B^3_{h,R}, \quad \| \hat{w}_{h,R} \|_2 \leq C_5\, hR \| \nabla \hat{w}_{h,R} \|_2\ .$$

Proof: Let K^* the reference element. For all $K \in \mathcal{T}_{h,R}$, there exists a linear function $F_K : K^* \to K$ defined by $F_K(x^*) = B_K x^* + b_K = x$. We denote w^* the function of $\boldsymbol{H}_0^1(K^*)$ defined by $w^*(x^*) = \hat{w}_{h,R}(x)$. We have

$$\| \hat{w}_{h,R} \|_2^2 \;=\; \sum_{K \in \mathcal{T}_{h,R}} \| \hat{w}_{h,R} \|_{2,K}^2 \;=\; \sum_{K \in \mathcal{T}_{h,R}} |\det(B_K)| \, \| w^* \|_{2,K^*}^2 \, .$$

Since $w^* \in \boldsymbol{H}_0^1(K^*)$, we may use the Poincaré inequality in K^*, i.e. there exists a constant C^* such that

$$\| w^* \|_{2,K^*} \;\leq C^* \, \| \nabla w^* \|_{2,K^*} \, .$$

Hence,

$$\| \hat{w}_{h,R} \|_2^2 \;\leq C^* \sum_{K \in \mathcal{T}_{h,R}} |\det(B_K)| \, \| \nabla w^* \|_{2,K^*}^2 \;\leq C^* \sum_{K \in \mathcal{T}_{h,R}} \|B_K\|^2 \, \| \nabla w^* \|_{2,K^*}^2 \, ,$$

where $\|B_K\| := \sqrt{B_K^T B_K}$ is the Frobenius norm of the matrix B_K. The value of $\|B_K\|$ for $K \in \mathcal{T}_{h,R} \cap U_j$ is of order $2^j h$, hence there exists a constant $C > 0$ independent of h and R such that $\|B_K\| \leq ChR$ for all $K \in \mathcal{T}_{h,R}$. $\square$

Remark 1 *We may deduce, using the interpolation inequality, that there exists a constant $C_6 > 0$ such that, for all $\hat{w}_{h,R} \in B_{h,R}^3$, we have*

$$\| \hat{w}_{h,R} \|_3 \;\leq C_6 (hR)^{1/2} \, \| \nabla \hat{w}_{h,R} \|_2 \, .$$

Lemma 2

$$\forall u_{h,R}, v_{h,R}, w_{h,R} \in V_{h,R}, \quad a_{1,h,R}(R_{1,h,R}S(w_{h,R}, u_{h,R}), R_{1,h,R}S(w_{h,R}, v_{h,R})) \\ \leq C_8 \alpha_1^{-1} \mathcal{R}e^2 \big((hR) + (hR)^{1/2} \, \| w_{h,R} \|^{(h,R)} \big)^2 \, \| u_{h,R} \|^{(h,R)} \, \| v_{h,R} \|^{(h,R)}.$$

Proof:

$$\begin{aligned}
&|a_{1,h,R}(R_{1,h,R}S(w_{h,R}, u_{h,R}), R_{1,h,R}S(w_{h,R}, v_{h,R}))| = |\langle S(w_{h,R}, u_{h,R}), R_{1,h,R}S(w_{h,R}, v_{h,R}) \rangle| \\
&\quad = \Big| \mathcal{R}e \int_{\Omega_{h,R}} D_1 u_{h,R} R_{1,h,R} S(w_{h,R}, v_{h,R}) \, dx \\
&\qquad + \mathcal{R}e \int_{\Omega_{h,R}} \big((w_{h,R} \cdot \nabla) u_{h,R} R_{1,h,R} S(w_{h,R}, v_{h,R}) \, dx + \frac{1}{2} (\nabla \cdot w_{h,R}) u_{h,R} R_{1,h,R} S(w_{h,R}, v_{h,R}) \big) \Big| \\
&\quad \leq \mathcal{R}e \; (\, \| D_1 u_{h,R} \|_2 \; \| R_{1,h,R} S(w_{h,R}, v_{h,R}) \|_2 \\
&\qquad + \| w_{h,R} \|_6 \; \| \nabla u_{h,R} \|_2 \; \| R_{1,h,R} S(w_{h,R}, v_{h,R}) \|_3 \\
&\qquad + \| \nabla \cdot w_{h,R} \|_2 \; \| u_{h,R} \|_6 \; \| R_{1,h,R} S(w_{h,R}, v_{h,R}) \|_3 \,) \\
&\quad \leq \mathcal{R}e \Big(\; \| u_{h,R} \|^{(h,R)} \, \| R_{1,h,R} S(w_{h,R}, v_{h,R}) \|_2 \\
&\qquad + \; 2C_1 \, \| u_{h,R} \|^{(h,R)} \, \| w_{h,R} \|^{(h,R)} \, \| R_{1,h,R} S(w_{h,R}, v_{h,R}) \|_3 \Big) \, .
\end{aligned}$$

Applying Lemma 1 and Remark 1, we obtain:

$$|a_{1,h,R}(R_{1,h,R}S(w_{h,R}, u_{h,R}), R_{1,h,R}S(w_{h,R}, v_{h,R}))| \\ \leq \mathcal{R}e\big(C_5 hR \, \| u_{h,R} \|^{(h,R)} + 2C_1 C_6 (hR)^{1/2} \, \| u_{h,R} \|^{(h,R)} \, \| w_{h,R} \|^{(h,R)} \big) \, \| \nabla R_{1,h,R} S(w_{h,R}, v_{h,R}) \|_2 \, . \quad (33)$$

It follows from the coercivity of the bilinear form $a_{1,h,R}$ and the preceding result (33) that

$$\| \nabla R_{1,h,R} S(w_{h,R}, v_{h,R}) \|_2^2 \;\leq \alpha_1^{-1} a_{1,h,R}(R_{1,h,R}S(w_{h,R}, v_{h,R}), R_{1,h,R}S(w_{h,R}, v_{h,R})) \\ \leq \alpha_1^{-1} \max(C_5, 2C_1 C_6) \mathcal{R}e\big((hR) \, \| v_{h,R} \|^{(h,R)} + (hR)^{1/2} \, \| v_{h,R} \|^{(h,R)} \, \| w_{h,R} \|^{(h,R)} \big) \, \| \nabla R_{1,h,R} S(w_{h,R}, v_{h,R}) \|_2 \, .$$

Consequently, we obtain the following estimate:

$$\| \nabla R_{1,h,R} S(w_{h,R}, v_{h,R}) \|_2 \;\leq \max(C_6, 2C_1 C_2) \alpha_1^{-1} \mathcal{R}e\big(hR \, \| v_{h,R} \|^{(h,R)} + (hR)^{1/2} \, \| v_{h,R} \|^{(h,R)} \, \| w_{h,R} \|^{(h,R)} \big). \quad (34)$$

Inserting (34) in (33), we have, for $C_8 = \max(C_5, 2C_1C_6)^2$,

$$\begin{aligned} &a_{1,h,R}(R_{1,h,R}S(w_{h,R},u_{h,R}),R_{1,h,R}(w_{h,R},v_{h,R})) \\ &\leq C_8\alpha_1^{-1}\mathcal{R}e^2\left(hR+(hR)^{1/2}\parallel w_{h,R}\parallel^{(h,R)}\right)^2 \parallel u_{h,R}\parallel^{(h,R)}\parallel v_{h,R}\parallel^{(h,R)}. \quad \square \end{aligned}$$

Lemma 3 *There exists a constant $\mathcal{C}>0$ independent of h, R and $\mathcal{R}e$ such that*

$$\forall p_{h,R}, q_{h,R} \in Q_{h,R}, \quad c_{h,R}(p_{h,R},q_{h,R}) \leq \mathcal{C} \parallel p_{h,R}\parallel_2 \ \parallel q_{h,R}\parallel_2 . \tag{35}$$

Proof: For all $p_{h,R}, q_{h,R} \in Q_{h,R}$,

$$|a_{2,h,R}(R_{2,h,R}\nabla p_{h,R}, R_{2,h,R}\nabla q_{h,R})| = |(p_{h,R}, \nabla\cdot(R_{2,h,R}\nabla q_{h,R}))| \leq \parallel p_{h,R}\parallel_2 \ \parallel \nabla R_{2,h,R}(\nabla q_{h,R})\parallel_2 .$$

Since

$$\parallel \nabla R_{2,h,R}(\nabla q_{h,R})\parallel_2^2 \ \leq \alpha_2^{-1} a_{2,h,R}(R_{2,h,R}\nabla p_{h,R}, R_{2,h,R}\nabla q_{h,R}) \leq \alpha_2^{-1}\parallel q_{h,R}\parallel_2 \ \parallel \nabla R_{2,h,R}(\nabla q_{h,R})\parallel_2 ,$$

we have

$$\parallel \nabla R_{2,h,R}(\nabla q_{h,R})\parallel_2 \ \leq \alpha_2^{-1}\parallel q_{h,R}\parallel_2 ,$$

and

$$|a_{2,h,R}(R_{2,h,R}\nabla p_{h,R}, R_{2,h,R}\nabla q_{h,R})| \leq \alpha_2^{-1}\parallel q_{h,R}\parallel_2 \ \parallel p_{h,R}\parallel_2 . \quad \square$$

Finally, we summarize all the results obtained:

$$\begin{aligned} &\forall u_{h,R}, v_{h,R}, w_{h,R}, \quad a_{h,R}^{(+)}(w_{h,R})(u_{h,R},v_{h,R}) \leq \ \mathcal{A}_+ \parallel u_{h,R}\parallel^{(h,R)} \parallel v_{h,R}\parallel^{(h,R)}, \\ &\text{where } \ \mathcal{A}_+ = C\left(1+\mathcal{R}e\ R+\alpha_1^{-1}\mathcal{R}e^2\big((hR)+(hR)^{1/2}\parallel w_{h,R}\parallel^{(h,R)}\big)^2\right). \end{aligned} \tag{36}$$

Since $a_{1,h,R}(R_{1,h,R}S(w_{h,R},u_{h,R}), R_{1,h,R}S(w_{h,R},u_{h,R})) \geq 0$, we have

$$\forall u_{h,R}, w_{h,R} \in V_{h,R}, \quad a_{h,R}^{(+)}(w_{h,R})(u_{h,R},u_{h,R}) \geq \alpha \ \left(\parallel u_{h,R}\parallel^{(h,R)}\right)^2 , \tag{37}$$

for $\alpha = 1$.

$$\begin{aligned} &\forall u_{h,R}, v_{h,R}, w_{h,R} \in V_{h,R}, \quad a_{h,R}^{(-)}(w_{h,R})(u_{h,R},v_{h,R}) \leq \ \mathcal{A}_- \parallel u_{h,R}\parallel^{(h,R)} \parallel v_{h,R}\parallel^{(h,R)}, \\ &\text{where } \ \mathcal{A}_- = C\mathcal{R}e\left(R+R^{1/2}\parallel w_{h,R}\parallel^{(h,R)}\right). \end{aligned} \tag{38}$$

There is a constant $\mathcal{B}>0$ such that

$$\forall u_{h,R} \in V_{h,R}, p_{h,R} \in Q_{h,R}, \quad b_{h,R}(u_{h,R},p_{h,R}) \leq \mathcal{B}\parallel p_{h,R}\parallel_2 \ \parallel u_{h,R}\parallel^{(h,R)}. \tag{39}$$

This discretization is well–adapted to our exterior problem if the finite element spaces satisfy a compatibility condition, also called generalized inf–sup condition with a coefficient independent of h and R. This means that the system is uniformly coercive, and the generalized inf–sup condition is given by:

Lemma 4 *There exists a constant $\gamma>0$ such that*

$$\forall q_{h,R} \in Q_{h,R}, \quad \sup_{v_{h,R}\in V_{h,R}} \frac{b_{h,R}(v_{h,R},q_{h,R})}{\parallel v_{h,R}\parallel^{(h,R)}} + c_{h,R}(q_{h,R},q_{h,R})^{1/2} \geq \gamma \parallel q_{h,R}\parallel_2 . \tag{40}$$

Proof : We know that the Babuska–Brezzi inequality is satisfied for the mixed finite elements spaces called P1+bubbles -P1 with a constant independent of h and R (see [8]). This means that there exists a constant $\beta>0$ such that $\forall h>0, \forall R>0$ satisfying (10), we have:

$$\forall q_{h,R} \in Q_{h,R}, \quad \sup_{\substack{v_{h,R}\in V_{h,R} \\ \hat{v}_{h,R}\in B^3_{h,R}}} \frac{b_{h,R}(v_{h,R}+\hat{v}_{h,R},q_{h,R})}{\parallel v_{h,R}+\hat{v}_{h,R}\parallel^{(h,R)}} \geq \beta \parallel q_{h,R}\parallel_2 . \tag{41}$$

Rebollo [17] proved that for all $v_{h,R} \in V_{h,R}$, for all $\hat{v}_{h,R} \in \boldsymbol{B}^3_{h,R}$, we have

$$|v_{h,R} + \hat{v}_{h,R}|_1^2 \geq 2\left(|v_{h,R}|_1^2 + |\hat{v}_{h,R}|_1^2\right).$$

Since $\hat{v}_{h,R} = 0$ on $\Gamma_{h,R}$, we obtain the following inequality:

$$\forall v_{h,R} \in V_{h,R}, \forall \hat{v}_{h,R} \in B^3_{h,R}, \quad \| v_{h,R} + \hat{v}_{h,R} \|^{(h,R)} \geq \sqrt{2}\left(\| v_{h,R} \|^{(h,R)} + \| \hat{v}_{h,R} \|^{(h,R)} \right). \tag{42}$$

Combining (42) and (41), we obtain

$$\begin{aligned}\beta \| q_{h,R} \|_2 &\leq \sup_{\substack{v_{h,R}\in V_{h,R}\\ \hat{v}_{h,R}\in B^3_{h,R}}} \frac{b_{h,R}(v_{h,R}+\hat{v}_{h,R}, q_{h,R})}{\| v_{h,R}+\hat{v}_{h,R} \|^{(h,R)}} \leq \sup_{\substack{v_{h,R}\in V_{h,R}\\ \hat{v}_{h,R}\in B^3_{h,R}}} \frac{b_{h,R}(v_{h,R}, q_{h,R})}{\| v_{h,R}+\hat{v}_{h,R} \|^{(h,R)}} + \sup_{\substack{v_{h,R}\in V_{h,R}\\ \hat{v}_{h,R}\in B^3_{h,R}}} \frac{b_{h,R}(\hat{v}_{h,R}, q_{h,R})}{\| v_{h,R}+\hat{v}_{h,R} \|^{(h,R)}} \\ &\leq \sqrt{2} \sup_{\substack{v_{h,R}\in V_{h,R}\\ \hat{v}_{h,R}\in B^3_{h,R}}} \frac{b_{h,R}(v_{h,R}, q_{h,R})}{\| v_{h,R} \|^{(h,R)}} + \sqrt{2} \sup_{\substack{v_{h,R}\in V_{h,R}\\ \hat{v}_{h,R}\in B^3_{h,R}}} \frac{b_{h,R}(\hat{v}_{h,R}, q_{h,R})}{\| \hat{v}_{h,R} \|^{(h,R)}}.\end{aligned}$$

Using (18), we have

$$\begin{aligned}\sup_{\substack{v_{h,R}\in V_{h,R}\\ \hat{v}_{h,R}\in B^3_{h,R}}} \frac{b_{h,R}(\hat{v}_{h,R}, q_{h,R})}{\| \hat{v}_{h,R} \|^{(h,R)}} &= \sup_{\substack{v_{h,R}\in V_{h,R}\\ \hat{v}_{h,R}\in B^3_{h,R}}} \frac{a_{2,h,R}(R_{2,h,R}(\nabla q_{h,R}), \hat{v}_{h,R})}{| \hat{v}_{h,R} |_1} \\ &\leq B_2 \, | R_{2,h,R}(\nabla q_{h,R}) |_1 = \frac{B_2}{\sqrt{\alpha_2}} a_{2,h,R}(R_{2,h,R}(\nabla q_{h,R}), R_{2,h,R}(\nabla q_{h,R}))^{1/2}.\end{aligned}$$

Hence, Lemma 4 is satisfied with

$$\gamma = \frac{\beta}{\sqrt{2}\max\left(1, \frac{B_2}{\sqrt{\alpha_2}}\right)}. \quad \square$$

4 Preconditioning for the Oseen system

We consider the Oseen system (27) where $w_{h,R}$ is a given function in $V_{h,R}$. We denote $k_{h,R}$ the dimension of the finite element space $V_{h,R}$ associated to the velocity and $m_{h,R}$ the dimension of the finite elements space $Q_{h,R}$ associated to the pressure. We denote $(\varphi_i)_{1\leq i\leq k_{h,R}}$ and $(\psi_j)_{1\leq j\leq m_{h,R}}$ the basis functions of $V_{h,R}$ and $Q_{h,R}$. We associate the functions $u_{h,R}, v_{h,R} \in V_{h,R}$, with the vectors $U, V \in \mathbb{R}^{k_{h,R}}, P, Q \in \mathbb{R}^{m_{h,R}}$ such that $u_{h,R} = \sum_{i=1}^{k_{h,R}} U_i\varphi_i$, $v_{h,R} = \sum_{i=1}^{k_{h,R}} V_i\varphi_i$, $p_{h,R} = \sum_{j=1}^{m_{h,R}} P_i\psi_j$ and $q_{h,R} = \sum_{j=1}^{m_{h,R}} Q_i\psi_j$. We define the matrices $\boldsymbol{A}, \boldsymbol{B}, \boldsymbol{E}, \boldsymbol{V}, \boldsymbol{Q}$ and the vectors F and G by:

$$(\boldsymbol{A}_+)_{i,j} = a^{(+)}_{h,R}(w_{h,R})(\varphi_j, \varphi_i), \quad (\boldsymbol{A}_-)_{i,j} = a^{(-)}_{h,R}(w_{h,R})(\varphi_j, \varphi_i), \quad \boldsymbol{B}_{i,j} = b_{h,R}(\varphi_j, \psi_i),$$

$$\boldsymbol{E}_{i,j} = c_{h,R}(\psi_j, \psi_i), \quad \boldsymbol{V}_{i,j} = (\varphi_j, \varphi_i)_{h,R}, \quad \boldsymbol{Q}_{i,j} = (\psi_j, \psi_i)$$

$$F_i = \langle f, \varphi_i \rangle, \quad G_i = \langle g, \psi_i \rangle.$$

We denote $\boldsymbol{A} := \boldsymbol{A}_+ + \boldsymbol{A}_-$ for the convection–diffusion matrix. The variational formulation of (27) may be written as the following linear system

$$\begin{pmatrix} \boldsymbol{A} & \boldsymbol{B}^T \\ \boldsymbol{B} & -\boldsymbol{E} \end{pmatrix} \begin{pmatrix} U \\ P \end{pmatrix} = \begin{pmatrix} F \\ G \end{pmatrix}, \tag{43}$$

where $\boldsymbol{E}$ is symmetric positive semi–definite. The influence of the preconditioner

$$\begin{pmatrix} \boldsymbol{A} & \boldsymbol{0} \\ \boldsymbol{B}^T & \boldsymbol{Q} \end{pmatrix} \tag{44}$$

is known [4] for such saddle–point problems when the domain is bounded. We will apply these results to our truncated problem.

It is proved in [4] that, if (40) is satisfied, the spectrum bounds of the preconditioned problem are known. They are given by:

Theorem 1 *The eigenvalues of the problem (43) preconditioned by (44) are included in the rectangular domain*

$$\left[\frac{\gamma^2}{2}\min(1,\alpha(\mathcal{A}_+^2+\mathcal{A}_-^2)^{-1}),(\frac{\mathcal{B}^2}{\alpha}+\mathcal{C})\right]\times\left[-\frac{\mathcal{B}^2}{2\alpha},\frac{\mathcal{B}^2}{2\alpha}\right], \tag{45}$$

where γ is the constant defined in the LBB condition (40) and $\mathcal{A}_+$, $\mathcal{A}_-$, $\mathcal{B}$, $\mathcal{C}$, α are the coercivity and continuity constants of the bilinear forms $a_{h,R}^{(+)}, a_{h,R}^{(-)}, b_{h,R}, c_{h,R}$ defined in (36), (38),(39), (35) and (37).

We suppose that there exists a constant μ such that $hR \leq \mu$ (this inequality appears naturally when we compute the discretization error [7]). If we denote C_1, C_2, C_3 et C_4 four constants independent of h, R and $\mathcal{R}e$, it follows that the eigenvalues of the preconditioned problem are included in the rectangular box:

$$\begin{aligned}&\left[C_1\min\left(1,m(R,\mathcal{R}e,w,\mu)^{-1}\right),C_4\right]\times\left[-\frac{1}{2},\frac{1}{2}\right]\\ &\text{with}\quad m(R,\mathcal{R}e,w,\mu)=C_2\left(1+\mathcal{R}e\;R+\mathcal{R}e^2\left(\mu+\mu^{1/2}\parallel w\parallel^{(h,R)}\right)^2\right)^2\\ &\qquad\qquad+C_3\mathcal{R}e^2\left(R+R^{1/2}\parallel w\parallel^{(h,R)}\right)^2.\end{aligned} \tag{46}$$

This means that the eigenvalues are independent of the mesh size, but depend on the truncation radius R.

We aim to know the asymptotic behavior of the spectrum bounds in function of $\mathcal{R}e$ and R. Suppose that $\exists\eta>0$ such that $\parallel w\parallel^{(h,R)}<\eta$. Hence, if $\mathcal{R}e$ is fixed, the domain takes the form

$$\left[\tilde{C}_1\min(1,\eta R^{-2}),\tilde{C}_2\right]\times\left[-\frac{1}{2},\frac{1}{2}\right], \tag{47}$$

where $\tilde{C}_1$ and $\tilde{C}_2$ depend on $\mathcal{R}e$. If R is fixed, we obtain this rectangular box:

$$\left[\bar{C}_1\min(1,\eta\mathcal{R}e^{-4}),\bar{C}_2\right]\times\left[-\frac{1}{2},\frac{1}{2}\right], \tag{48}$$

where $\bar{C}_1$ and $\bar{C}_2$ depend on R. This domain can be reduced to

$$\left[\bar{C}_1\min(1,\eta\mathcal{R}e^{-2}),\bar{C}_2\right]\times\left[-\frac{1}{2},\frac{1}{2}\right], \tag{49}$$

if we drop the velocity stabilization term.

5 Numerical results

5.1 Description of the tests

We consider two situations

a) Polynomial test case.

We choose as test function

$$\begin{aligned}u_1(x)&=(y-z)\Lambda(x)\\ u_2(x)&=(z-x)\Lambda(x)\\ u_3(x)&=(x-y)\Lambda(x)\\ \pi(x)&=10(|x|^{-3}-2|x|^{-4}+|x|^{-5}).\end{aligned} \tag{50}$$

with

$$\Lambda(x)=40|x|^{-3}(1-3|x|^{-1}+3|x|^{-2}-|x|^{-3}).$$

We define f by

$$-\triangle u+\mathcal{R}e\;D_1u+\mathcal{R}e'u\cdot\nabla u+\nabla p=f,$$

where the additional parameter $\mathcal{R}e'$ allows to include the situation $\mathcal{R}e'=0$, corresponding to the Oseen system

$$-\triangle u+\mathcal{R}e\;D_1u+\nabla p=f.$$

Then, f reads:

$$
\begin{aligned}
f_0(x) &= -(y-z)\Gamma_4(x) + \mathcal{R}e\,(y-z)x\Gamma_3(x) + \mathcal{R}e'\Lambda(x)^2(z+y-2x) + x\Gamma_2(x),\\
f_1(x) &= -(z-x)\Gamma_4(x) + \mathcal{R}e\,(z-x)x\Gamma_3(x) - \mathcal{R}e\,\Lambda(x) + \mathcal{R}e'\Lambda(x)^2(x+z-2y) + y\Gamma_2(x),\\
f_3(x) &= -(x-y)\Gamma_4(x) + \mathcal{R}e\,(x-y)x\Gamma_3(x) + \mathcal{R}e\Lambda(x) + \mathcal{R}e'\Lambda(x)^2(x+y-2z) + z\Gamma_2(x),\\
f_4(x) &= 0,
\end{aligned}
$$

where

$$
\begin{aligned}
\Gamma_2(x) &= 10|x|^{-5}(-3+8|x|^{-1}-5|x|^{-2}),\\
\Gamma_4(x) &= 240|x|^{-6}(-2+5|x|^{-1}-3|x|^{-2}),\\
\Gamma_3(x) &= 120|x|^{-5}(-1+4|x|^{-1}-5|x|^{-2}+2|x|^{-3}).
\end{aligned}
$$

This test-function satisfy the homogeneous Dirichlet boundary condition and is chosen such that $\nabla \cdot (u_1, u_2, u_3)^T = 0$.

b) Physical test case
We choose as right-hand side $f = 0$. This implies that the fluid does not interact with any field force, and in particular, that we neglect the gravity force. We take as Dirichlet boundary condition $u_{|\partial\Omega} = -e_1$.

The numerical tests are done in C++ using Lapack, Blas and SparseLib++ libraries. Computations were performed in the University of Lyon I.

5.2 Eigenvalues of the preconditioned problem

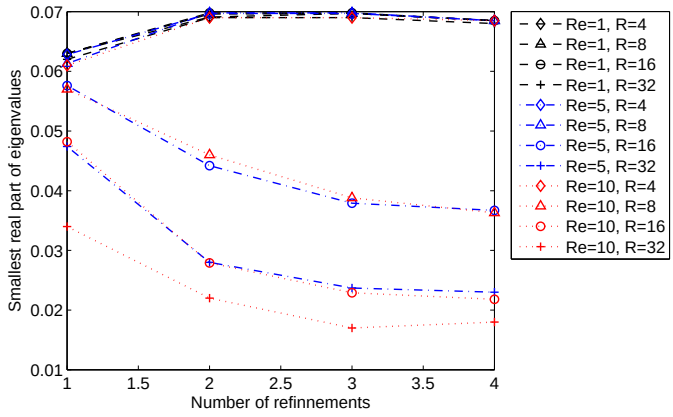

Figure 2: Real lower bound of the spectrum in function of the number of refinements

At first, we consider the test case a) with $\mathcal{R}e' = 0$. Using IRA ('Implicit Restarted Arnoldi') algorithm [**?**], we compute the smallest and largest real part of eigenvalues of the non–preconditioned problem, and next those of the preconditioned problem. In Table 1, first values (in roman) represent the higher real part of eigenvalues. Second ones (in italic) correspond to the smallest real part. We observe that the upper bound of the spectrum grows exponentially with R and the lower bound decreases with h. This operator is so ill–conditioned that we must stop the computation of eigenvalues. Indeed, Arnoldi method diverges for smaller values of h.

We observe in Table 2 that, when the convection is moderate (small Reynolds number or small truncation radius), the smallest real part of eigenvalues does not decrease (for example, $R = 4$ or $\mathcal{R}e = 1$) when we refine the mesh. On the contrary, if we consider the results for $\mathcal{R}e = 10$ and $R = 32$, we note that the smallest real part of eigenvalues decreases for the three first refinements. However, if we observe Figure 2, it is obvious that the smallest real part of eigenvalues has a lower bound independent of h. The decay observed during the first refinements does not contradict the theory: Indeed, inverse inequalities are some better estimates than Sobolev injections when h is large and the theoretical estimates are not optimal in this case. For this reason, we may expect a decay with h up to a threshold. Moreover, the lower bound decreases more slowly than the theoretical results predict when $\mathcal{R}e$ increases. We have already observed this behavior for the dependence on the Reynolds number when we had considered the 3D-driven cavity benchmark (see [4]). The decay with R of the smallest

	R=4	R=8	R=16	R=32
$h = 1/2, \quad \mathcal{R}e = 1$	2.39068	13.05051	71.09987	407.19287
	0.01142	*0.01136*	*0.01136*	*0.01136*
$h = 1/2, \quad \mathcal{R}e = 10$	0.80746	3.87074	26.54404	201.18800
	0.01136	*0.01134*	*0.01134*	*0.01134*
$h = 1/4, \quad \mathcal{R}e = 1$	1.43347	4.98361	35.00725	238.03966
	0.06355	*0.0014056*	*0.0014057*	*0.0015853*
$h = 1/4, \quad \mathcal{R}e = 10$	0.42256	2.560515	14.669986	82.443984
	0.06126	*0.0014021*	*0.0014023*	*0.0014948*

Table 1: Eigenvalues of the Schur Complement. $w_{h,R} = 0$. No preconditioning, no velocity stabilization term. In roman, the upper bound. In Italic, the lower bound.

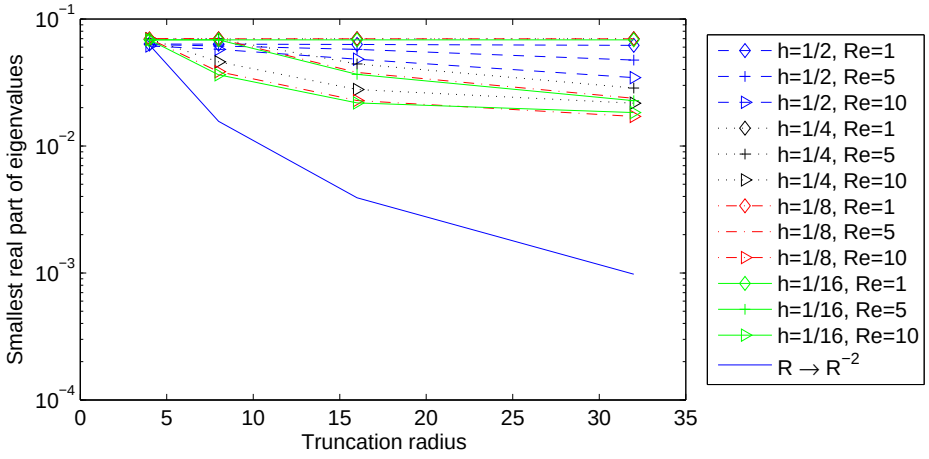

Figure 3: Lower bound of the spectrum in function of the truncation radius

		R=4	R=8	R=16	R=32
$h = 1/2,$	$\mathcal{R}e = 1$	1.433473	1.434075	1.4340454	1.4340586
		0.063548	*0.063357*	*0.062993*	*0.061958*
$h = 1/2,$	$\mathcal{R}e = 5$	1.395297	1.396560	1.396773	1.3968181
		0.0628294	*0.0613446*	*0.057675*	*0.04742464*
$h = 1/2,$	$\mathcal{R}e = 10$	1.379707	1.381793	1.3820807	1.382141
		0.061256	*0.057675*	*0.0482294*	*0.034518*
$h = 1/4,$	$\mathcal{R}e = 1$	1.27322	1.2732836	1.2732997	1.27329999
		0.06918	*0.069618*	*0.069804*	*0.06988896*
$h = 1/4,$	$\mathcal{R}e = 5$	1.0572641	1.057342	1.05721083	1.057198
		0.0696944	*0.0698615*	*0.0442464*	*0.0286589*
$h = 1/4,$	$\mathcal{R}e = 10$	0.93265	0.933576	0.934647	0.934605
		0.069777	*0.046009*	*0.0278978*	*0.0217531*
$h = 1/8,$	$\mathcal{R}e = 1$	1.1194181	1.1942614	1.19426134	1.194213
		0.0697365	*0.0697829*	*0.0698052*	*0.0698393*
$h = 1/8,$	$\mathcal{R}e = 5$	1.0208700	1.0208712	1.0208769	1.0208773
		0.0697584	*0.0698143*	*0.0379934*	*0.0236745*
$h = 1/8,$	$\mathcal{R}e = 10$	0.888447	0.888533	0.8885484	0.888555
		0.0697829	*0.03844003*	*0.022875*	*0.0171925*
$h = 1/16,$	$\mathcal{R}e = 1$	1.106324	1.1063514	1.1063513	1.1063513
		0.068540	*0.0685579*	*0.06856596*	*0.0685715*
$h = 1/16,$	$\mathcal{R}e = 5$	1.0076067	1.0076067	1.0076067	1.0076067
		0.0685418	*0.0685594*	*0.0366970*	*0.0227263*
$h = 1/16,$	$\mathcal{R}e = 10$	0.09176969	0.09176969	0.0917697	0.091769692
		0.06854277	*0.036339*	*0.0218450*	*0.01837461*

Table 2: Eigenvalues of $\boldsymbol{Q}^{-1}\boldsymbol{S}$, $w_{h,R} = 0$. No velocity stabilization. In roman, the upper bound. In italic, the lower bound.

real part of eigenvalues is plotted in Figure 3 and we observe that the decay is sublinear. To better understand the role of the parameters $\mathcal{R}e$ and R, we plot the complete spectrum of $\boldsymbol{Q}^{-1}\boldsymbol{S}$ for several values of R and $\mathcal{R}e$ when $h = 1/4$. We see in Figure 4 that increasing the Reynolds number $\mathcal{R}e$ acts simultaneously on the real and imaginary bound of the spectrum: Indeed, $\mathcal{R}e$ acts naturally on the convective part of $\boldsymbol{A}$, but also on the diffusive part through the approximate boundary condition contribution. On the contrary, the radius R plays an other role : we observe in Figure 5 that the imaginary bound is unchanged when R increases but the number of eigenvalues with a small real part increases when R grows.

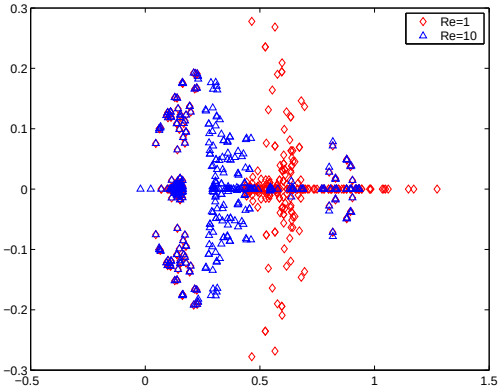

Figure 4: Spectrum of $\boldsymbol{Q}^{-1}\boldsymbol{S}$ for $R = 8$.

Now, set $\mathcal{R}e' = \mathcal{R}e$. We build the convection–diffusion matrix when the advective term is the solution u defined in (50). We add the stabilization term with stabilization parameters $A = P = 1$. Table 3 shows that

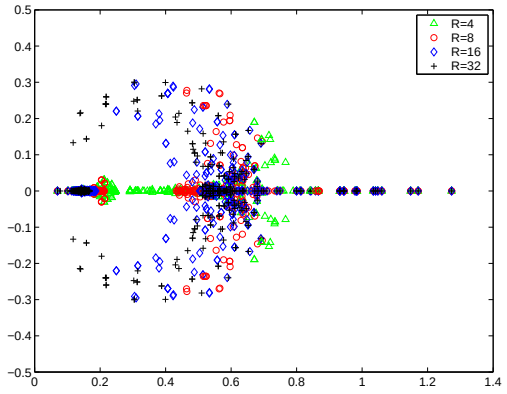

Figure 5: Spectrum of $\boldsymbol{Q}^{-1}\boldsymbol{S}$ for $\mathcal{R}e = 1$.

the upper bound of the spectrum decays with $\mathcal{R}e$ when h becomes small. These results are analogous to those obtained in bounded cases (see [4]).

	R=4	R=8	R=16	R=32
$h = 1/2, \quad \mathcal{R}e = 1$	1.41135	1.411135	1.411112	1.411126
	0.062800	*0.062748*	*0.062740*	*0.061885*
$h = 1/2, \quad \mathcal{R}e = 5$	1.36556	1.365648	1.365650	1.36548
	0.059303	*0.058197*	*0.056417*	*0.046989*
$h = 1/2, \quad \mathcal{R}e = 10$	1.37526	1.375736	1.375704	1.375695
	0.058401	*0.053160*	*0.049435*	*0.034597*
$h = 1/4, \quad \mathcal{R}e = 1$	1.248038	1.247578	1.247549	1.247549
	0.069733	*0.069968*	*0.699687*	*0.069967*
$h = 1/4, \quad \mathcal{R}e = 5$	1.013431	1.013309	1.013308	1.013312
	0.072150	*0.070182*	*0.047684*	*0.034597*
$h = 1/4, \quad \mathcal{R}e = 10$	0.989509	0.989459	0.989460	0.989480
	0.057357	*0.034037*	*0.027707*	*0.021960*
$h = 1/8, \quad \mathcal{R}e = 1$	1.188877	1.188412	1.188390	1.188390
	0.069884	*0.070112*	*0.070007*	*0.069911*
$h = 1/8, \quad \mathcal{R}e = 5$	1.042867	1.042867	1.042867	1.042867
	0.039913	*0.038175*	*0.038167*	*0.024657*
$h = 1/8, \quad \mathcal{R}e = 10$	0.921047	0.899542	0.899547	0.899540
	0.029208	*0.028095*	*0.020501*	*0.017386*

Table 3: Eigenvalues of $\boldsymbol{Q}^{-1}\boldsymbol{S}$. Polynomial convection defined in a). Velocity stabilization with $A = P = 1$. In roman, the upper bound. In italic, the lower bound.

5.3 Performances

We solve the convection–diffusion problem with a GMRES(30) preconditioned by ILU(0) factorization. The matrix $\boldsymbol{Q}$ is replaced by a mass–lumping of $\boldsymbol{Q}$. At first, we drop the velocity stabilization and we study only the linear problem obtained when we put $\mathcal{R}e' = 0$. On the complete system, we apply a FGMRES without restart until the residual decreases by a factor of 10^{-5}. We do not restart because the iteration count depends on the number of restarts. Table 4 gives us the FGMRES iteration count until convergence. We call "polynomial right-hand side" the test described in a) and "zero right-hand side" the Oseen problem with $w_{h,R} = 0$, $f = 0$ and $u = -e_1$ on $\partial\Omega$.

We observe in the columns of Table 4 corresponding to the polynomial right–hand side case that FGMRES iteration number grows with the number of refinements. This phenomenon is due to the right–hand side condition number, which increases with $\mathcal{R}e$ and R. Indeed, looking at the three last columns of Table 4, we note that the iteration count is bounded when h decays if $\mathcal{R}e$ and R are small (the upper bound seems attained

			polynomial right–hand side			zero right–hand side		
h	R	Size	$\mathcal{R}e = 1$	$\mathcal{R}e = 5$	$\mathcal{R}e = 10$	$\mathcal{R}e = 1$	$\mathcal{R}e = 5$	$\mathcal{R}e = 10$
1/2	4	312	18	18	18	27	25	24
1/2	8	440	19	20	20	27	27	26
1/2	16	568	23	24	24	29	30	33
1/2	32	696	27	28	30	32	37	37
1/2	64	824	31	34	48	37	42	40
1/4	4	2152	25	27	28	36	37	37
1/4	8	3128	29	33	33	38	48	50
1/4	16	4104	35	41	40	47	59	68
1/4	32	5080	43	49	51	52	75	79
1/4	64	6056	56	63	103	64	89	87
1/8	4	16200	30	38	42	42	75	64
1/8	8	23912	37	47	56	51	78	88
1/8	16	31624	46	66	75	76	105	117
1/8	32	39336	62	88	99	78	126	159
1/8	64	47048	83	121	177	99	194	198
1/16	4	131522	35	48	62	40	56	70
1/16	8	167592	42	64	84	45	73	95
1/16	16	249096	56	95	118	55	99	142
1/16	32	310600	83	140	156	74	148	189
1/16	64	372104	123	197	231	109	201	261

Table 4: FGMRES iteration count for the linearized problem

for $h = 1/8$). On the contrary, we do not observe this for higher values of $\mathcal{R}e$ and R and we believe that more refinements are necessary to obtain the same behavior. Furthermore, do not forget that increasing R without refining the mesh implies that the mesh size is enormous in the last layer.

5.4 Nonlinear iterations

We use the "adaptive fixed point defect correction method" from Turek[20]: The stopping criterion for the nonlinear iterations is $\|\text{res}_{nonlin}\| \leq 10^{-3}$ where res_{nonlin} is the finite element residual. Each inner linear system is solved with a relative residual precision of 10^{-1}. Ev (resp Ep) corresponds to the approximate L^2-error on $B(0, s)$ for the velocity (resp. the pressure). it-nl is the number of nonlinear iterations and it-fgmres is the average number of FGMRES iterations. We neglect the velocity stabilization term and we fix $\mathcal{R}e = 1$.

The decay results for the discretization error conform to the results obtained by Deuring in [6] and [7]. Moreover, we observe that the nonlinear iteration count is independent of the mesh size h and of the truncation radius R. For the average number of FGMRES iterations, we plot the values in Figure 6. We observe that the iteration number grows more slowly when h^{-1} and R increase. We do not continue to refine the mesh, because if we do, the number of degres of freedom will exceed one million and will require huge computational power.

To study the behavior in function of the Reynolds number, we consider the more physical test case b). The results are presented in Table 6. Roman values correspond to the number of nonlinear iterations and italic values to the average number of FGMRES iterations. Similarly to the linear case, the number of FGMRES iterations grows then stagnates with the refinement number for the easier cases ($\mathcal{R}e = 1$ et $R = 4, 8$ or 16). For the other situations, we need more refinements to conclude. Moreover, we may observe the robustness of the quasi-Newton method in function of h and R. This remark implies that the difficulty remains in the resolution od the Oseen-type system, since the spectrum of the preconditioned problem depends on the convective term.

5.5 Representation of the solution

We plot[1] the solution of the physical test case. Figure 7 represents isolines for $\mathcal{R}e = 20$ and Figure 8 draws isovalues for the Euclidean norm of velocity in the plan $y = 0$. When observing the drag for $\mathcal{R}e = 20$ in Figure 8, we understand that it is impossible to consider that, for $\mathcal{R}e >> 20$, the solution decays on the truncation

[1]Figures are drawn using Paraview Software (http://www.paraview.org).

		R=4	R=8	R=16	R=32	R=64
h=1/2	d.o.f.	312	440	568	699	952
	Ev	0.54	0.36	0.28	0.26	0.25
	Ep	2.40	2.13	1.52	1.31	1.25
	it-nl	6	7	8	9	9
	it-fgmres	13.8	16.4	18.25	22	26.6
h=1/4	d.o.f.	2 152	3 128	4 104	5 080	7 032
	Ev	0.45	0.23	0.13	0.09	0.08
	Ep	1.84	1.16	0.64	0.48	0.45
	it-nl	7	9	10	11	11
	it-fgmres	25.7	29.2	32.4	45.3	62.6
h=1/8	d.o.f.	16 200	23 912	31 624	39 336	47 048
	Ev	0.41	0.19	0.08	0.035	0.022
	Ep	1.51	0.78	0.31	0.19	0.16
	it-nl	7	10	11	11	11
	it-fgmres	32.3	41.5	50.2	70.2	93.72
h=1/16	d.o.f.	131 522	167 592	249 096	310 600	372 014
	Ev	0.41	0.19	0.07	0.024	0.013
	Ep	1.40	0.67	0.23	0.13	0.14
	it-nl	7	9	10	10	10
	it-fgmres	39.1	46.5	58.4	82.7	104.7

Table 5: Nonlinear iterations, polynomial test case, $\mathcal{R}e = 1$

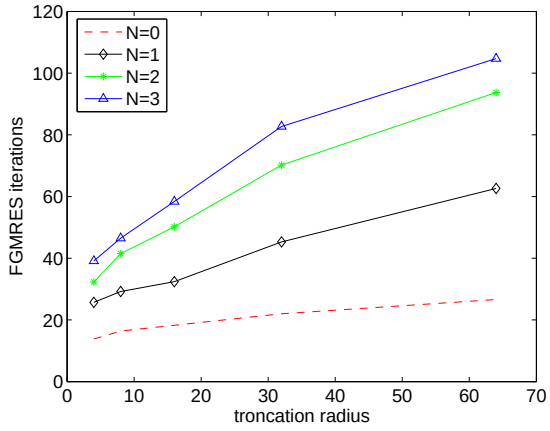

Figure 6: Average number of FGMRES iteration un function of R.

$\mathcal{R}e$	h	$R = 4$	$R = 8$	$R = 16$	$R = 32$	$R = 64$
1	1/2	5 - *15.4*	5 - *17.4*	5 - *20.8*	5 - *24.8*	5 - *33.2*
	1/4	5 - *33.8*	5 - *42*	5 - *54.6*	5 - *82.8*	5 - *137.2*
	1/8	5 - *52*	5 - *60.8*	5 - *93.6*	5 - *135.2*	5 - *257.8*
	1/16	5 - *59.6*	5 - *71*	5 - *98.2*	5 - *229.5*	5 - *356.6*
10	1/2	6 - *14.6*	6 - *18.7*	6 - *23.7*	6 - *27.3*	6 - *30.2*
	1/4	6 - *36.2*	6 - *46.8*	6 - *65.7*	6 - *78.5*	6 - *88.8*
	1/8	7 - *92.7*	7 - *163.4*	7 - *203.8*	6 - *208.3*	6 - *235.5*
	1/16	7 - *135.8*	7 - *254.8*	7 - *357.5*	7 - *412.1*	7- *581.1*

Table 6: Nonlinear iterations for the physical test case b)

radius for some reasonable values of R. For these values of $\mathcal{R}e$, we must consider the non-steady Navier–Stokes equations with other artificial boundary conditions.

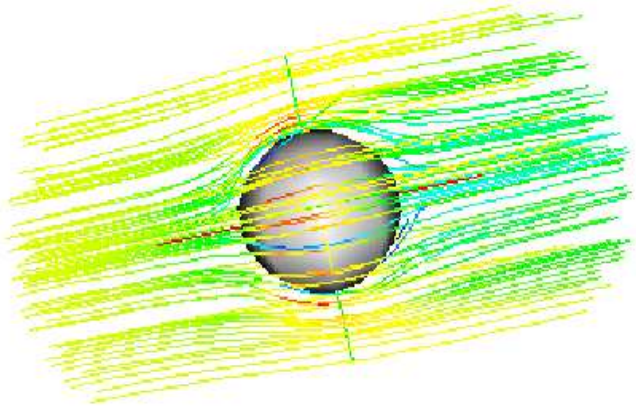

Figure 7: Isolines for $\mathcal{R}e = 20$.

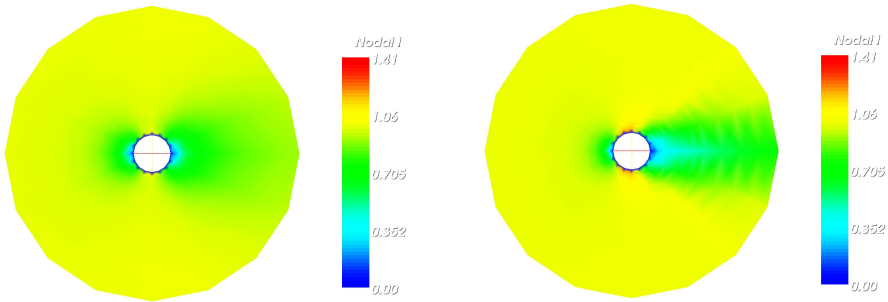

(a) Re=1

(b) Re=10

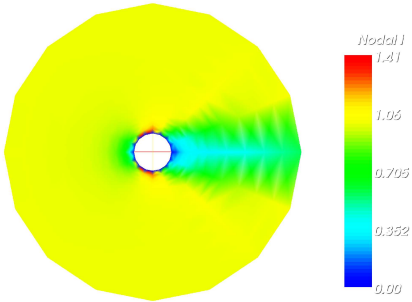

(c) Re=20

Figure 8: Isovalues of the velocity in the plan (xOz) with $R = 16$.

Acknowledgments

The author wish to thank Caterina Calgaro and Paul Deuring for their valuable comments.

References

[1] F. Alouges, J. Laminie, and S. M. Mefire. Exponential meshes and three-dimensional computation of a magnetic field. *Numer. Methods Partial Differential Equations*, 19(5):595–637, 2003.

[2] François Alouges. Computation of the demagnetizing potential in micromagnetics using a coupled finite and infinite elements method. *ESAIM Control Optim. Calc. Var.*, 6:629–647 (electronic), 2001.

[3] C. Calgaro, P Deuring, and D. Jennequin. Computation of 3d exterior stationary incompressible navier-stokes flowswith non-zero velocity at infinity. In *PAMM*, volume 3, pages 533 – 534, 2003.

[4] C. Calgaro, P Deuring, and D. Jennequin. A preconditioner for generalized saddle point problems: Application to 3d navier stokes equations. *Numer. Meth. in P.D.E.*, à paraître.

[5] Zhi-Hao Cao. Fast iterative solution of stabilized Navier-Stokes systems. *Appl. Math. Comput.*, 157(1):219–241, 2004.

[6] P. Deuring. A finite element method for computing 3d exterior stationary navier-stokes flows. i. stability and numerical test. Technical Report 244, LMPA, 2005.

[7] P. Deuring. A finite element method for computing 3d exterior stationary navier-stokes flows. ii. error estimates. Technical Report 245, LMPA, 2005.

[8] Paul Deuring. Finite element methods for the Stokes system in three-dimensional exterior domains. *Math. Methods Appl. Sci.*, 20(3):245–269, 1997.

[9] Paul Deuring. A stable mixed finite element method on truncated exterior domains. *RAIRO Modél. Math. Anal. Numér.*, 32(3):283–305, 1998.

[10] Paul Deuring and Stanislav Kračmar. Exterior stationary Navier-Stokes flows in 3D with non-zero velocity at infinity: approximation by flows in bounded domains. *Math. Nachr.*, 269/270:86–115, 2004.

[11] H. C. Elman and D. Silvester. Fast nonsymmetric iterations and preconditioning for navier-stokes equations. *SIAM J. Sci. Comput.*, 17:33–46, 1996.

[12] H. C. Elman, D. J. Silvester, and A. J. Wathen. Performance and analysis of saddle point preconditioners for the discrete steady-state navier-stokes equations. *Numer. Math.*, 90:665–688, 2002.

[13] V. Girault and P.A Raviart. *Finite element methods for Navier-Stokes equations*, volume 5 of *Springer Series in Computational Mathematics*. Springer-Verlag, Berlin, 1986. Theory and algorithms.

[14] C. I. Goldstein. The finite element method with nonuniform mesh sizes for unbounded domains. *Math. Comp.*, 36(154):387–404, 1981.

[15] D. Loghin. Analysis of preconditioned picard iterations for the navier-stokes equations. Technical Report 01/10, Oxford University, Numerical Ananlysis Group, 2001.

[16] D. Loghin and A. J. Wathen. Schur complement preconditioners for the navier-stokes equations. *Int. J. Numer. Meth. Fluids.*, 40:"403–412", 2002.

[17] T. C. Rebollo. A term by term stabilization algorithm for finite element solution of incompressible fluid flow problems. *Numer. Math.*, 79:"282–319", 1998.

[18] D. Silvester, H. Elman, D. Kay, and A. Wathen. Efficient preconditioning of the linearized navier-stokes equations for incompressible flow. *J. Comput. Appl. Math.*, 128:"261–279", 2001.

[19] Semyon V. Tsynkov. Numerical solution of problems on unbounded domains. A review. *Appl. Numer. Math.*, 27(4):465–532, 1998. Absorbing boundary conditions.

[20] Stefan Turek. *Efficient solvers for incompressible flow problems*, volume 6 of *Lecture Notes in Computational Science and Engineering*. Springer-Verlag, Berlin, 1999.

[21] A. Wathen, D.Loghin, D.Kay, H.C. Elman, and D. Silvester. A preconditioner for the 3d oseen equation, 2002.

[22] Lung An Ying. *Infinite element methods*. Peking University Press, Beijing, chinese edition, 1995. With a preface by Peter D. Lax.

A Stabilization terms

We will check that the relations given by Rebollo [17] to compute the stabilization terms satisfy the equations (17) and (18). Note that we modify Rebollo's formulations because we consider dimensionless Navier–Stokes equations. Let A and P two numerical constants and let $p \in (3, \infty)$. For $K \in \mathcal{T}_{h,R}$, the Péclet number is defined by

$$Pe_K = \mathcal{R}e \ \| (e_1 + w_{h,R})|_K \|_p \ diam\, K.$$

We have, for all $v_{h,R}, z_{h,R} \in V_{h,R}$,

$$a_{1,h}(v_{h,R}, z_{h,R}) = \sum_{K \in T_{h,R}} \frac{Vol(K)}{840^2 \tau_{1,K} \mid \hat{b}_K \mid_1^2} (\nabla v_{h,R}, \nabla z_{h,R})_K, \tag{51}$$

where the symbol $(\ ,\ )_K$ represents the scalar product $L^2(K)$ and

$$\tau_{1,K} = A \frac{h_K}{\mathcal{R}e \ \| (e_1 + w_{h,R})|_K \|_p} \min(P, Pe_k).$$

We observe that Ah_K^2 is a upper bound of $\tau_{1,K}$. For the lower bound, if $P \geq Pe_K$, we have $\tau_{1,K} \geq Ah_k^2$. If $P \leq Pe_K$, then

$$\tau_{1,K} \geq A \ \frac{h_K}{\mathcal{R}e} \ \frac{1}{\| w_{h,R} + e_1 \|_p}.$$

We may suppose that $h < 1$ since the diameter of the first layer is equal to 1. For $K \in U_j$, $h_K \equiv 2^j h$, hence we obtain that

$$\tau_{1,K} \geq A \ \frac{h_K^2}{2^J \mathcal{R}e} \ \frac{1}{\| w_{h,R} + e_1 \|_p} \geq AS \frac{h_K^2}{R\mathcal{R}e} \ \frac{1}{\| w_{h,R} + e_1 \|_p}.$$

Following [17, Lemma 5.2], we deduce that there are two constants η_1 and η_2 depending only on the regularity σ of the triangulation such that

$$\alpha_1 = \frac{\eta_2}{840^2 A} \quad \text{and} \quad B_{1,h,R} = \frac{\eta_1}{840^2 A} \max(1, \mathcal{R}e \ R \ \| w_{h,R} + e_1 \|_p \ ). \tag{52}$$

Contents

Unité de recherche INRIA Futurs
Parc Club Orsay Université - ZAC des Vignes
4, rue Jacques Monod - 91893 ORSAY Cedex (France)

Unité de recherche INRIA Lorraine : LORIA, Technopôle de Nancy-Brabois - Campus scientifique
615, rue du Jardin Botanique - BP 101 - 54602 Villers-lès-Nancy Cedex (France)
Unité de recherche INRIA Rennes : IRISA, Campus universitaire de Beaulieu - 35042 Rennes Cedex (France)
Unité de recherche INRIA Rhône-Alpes : 655, avenue de l'Europe - 38334 Montbonnot Saint-Ismier (France)
Unité de recherche INRIA Rocquencourt : Domaine de Voluceau - Rocquencourt - BP 105 - 78153 Le Chesnay Cedex (France)
Unité de recherche INRIA Sophia Antipolis : 2004, route des Lucioles - BP 93 - 06902 Sophia Antipolis Cedex (France)

Éditeur
INRIA - Domaine de Voluceau - Rocquencourt, BP 105 - 78153 Le Chesnay Cedex (France)
http://www.inria.fr
ISSN 0249-6399